GNSS Channel Coding Structures for Fast Acquisition Signals in Harsh Environment Conditions

Lorenzo Ortega, Charly Poulliat

Received <day> <Month>, <year> | Revised <day> <Month>, <year> | Accepted <day> <Month>, <year>

DOI: xxx/xxxx

ARTICLE TYPE

GNSS Channel Coding Structures for Fast Acquisition Signals in Harsh Environment Conditions.

Lorenzo Ortega*[1] | Charly Poulliat[2]

[1]IPSA, Toulouse, France
[2]IRIT, INP-ENSEEIHT, University of Toulouse, Toulouse, France

Correspondence
Lorenzo Ortega, This is sample corresponding address. Email: lorenzo.ortega@ipsa.fr

Abstract

In this article, we investigate on a new method to jointly design the navigation message with an error correcting scheme. This joint design exploits the "carousel" nature of the broadcasted navigation message and allows both: i) to reduce the Time To First Fix (TTFF) and ii) to enhance the error correcting performances under favorable and challenging channel conditions. We show that the joint design requires error correcting schemes characterized by Maximum Distance Separable (MDS) and the full diversity properties. Those error correcting codes are referred to as Root Low Density Parity Check (Root-LDPC) codes and they can efficiently operate on block varying channels, enabling the efficient and rapid recovery of information over possibly non ergodic channels. Finally, in order to ensure the data demodulation performance over harsh condition, we propose Root-LDPC codes endowed with the nested property, which allows to inherently adapt the channel coding rate depending on the number of received blocks. The proposed error correcting joint design is then simulated and compared with the well-known GPS L1C subframe 2 structure under several transmission scenarios. Simulations show that we can have some enhancement of the error correction performance and a reduction of the TTFF for some scenarios.

KEYWORDS
TTD, MDS, Full diversity, Nested Root-LDPC codes, Demodulation threshold, Protograph EXIT, Navigation message structure.

1 | INTRODUCTION

Precise position, navigation and timing information are demanded features in new applications such as Intelligent Transportation Systems (ITS), automated aircraft landing or autonomous unmanned ground/air vehicles. For these types of applications, the main source of positioning information is provided by Global Navigation Satellite Systems (GNSS) (Teunissen & Montenbruck, 2017), a technology which has attracted a lot of interest in the recent years and which requires to provided not only reliability and integrity but also authentication of legitimate transmission.

In recent years, the principal working groups in charge of the design of the new generation of GNSS signals have decided to include error correcting codes (i.e., such as low-density parity-check (LDPC) or convolutional codes (Galileo-ICD, 2016; GPS-L1C-ICD, 2021)) in order to enhance the data demodulation performance. Moreover, in recent works (Ortega et al., n.d. 2018a 2018b 2020; Schotsch et al., 2017), the interest for reducing the Time To First Fix (TTFF) in the GNSS system has motivated the design of novel channel coding schemes which aim to decrease the time to retrieve the Clock and Ephemerides Data (CED), also called Time To Data (TTD). Those schemes exploit the Maximum Distance Separable (MDS) (Boutros et al.,

2010) property in order to decode reliable data information as fast as possible. In Ortega et al. (2018b); Schotsch et al. (2017), channel coding schemes which exploit both serial concatenation and MDS property were proposed in order to reduce the TTD but also to improve the demodulation threshold of the CED. In addition, theses schemes combine error correcting techniques with error detecting techniques in order to ensure the robustness of the CED. However, as it has been shown in Ortega et al. (2020) that those channel coding schemes are not outage achieving error correcting schemes (Boutros et al., 2010). Hence, the data resilience can be degraded under harsh environments.

In order to enhance the error correction performance, a new methodology to design jointly the navigation message structure and the channel coding scheme has been proposed in Ortega et al. (2018a 2020). This method models the navigation message acquisition as a block fading channel with erasures (Biglieri et al., 1998). Thus, the navigation data and the redundant bits from the channel encoder are divided in different information blocks that can experience different channel conditions (i.e. each information block is affected by a different fading coefficient). In case of deep fading, the information block can be assumed missing (i.e. the information block is erased). In this context, the received navigation message can be modeled by: i) some information blocks received with errors and different average signal-to noise ratios and ii) some information blocks that are missing. Thanks to this novel co-design under the block fading channel with erasures, the condition to retrieve the CED when there are missing blocks was derived, yielding to the need of channel coding schemes with the MDS property. Moreover, thanks to the navigation message acquisition model, a second desired property was also introduced. This property, denoted as full diversity, allows to exploit the entire diversity of the channel improving the data demodulation under harsh environments. In Ortega et al. (2018a), a co-design of the message structure and the channel coding based on a regular Root-LDPC (Boutros et al., 2010) codes of rate $R = 1/2$ was proposed. This error correcting family achieves both MDS and the full diversity properties when applying the Min-sum or the Belief-propagation (BP) decoding algorithms, as long as the CED and the redundant data generated by the channel encoder are divided into two blocks. An extension of this work was proposed in Ortega et al. (2020). In this extension, an irregular Protograph Root-LDPC code of rate $R = 1/2$ was designed with the purpose of improving the error correction capabilities (i.e. convergence and demodulation threshold) under the BP algorithm. Furthermore, two independent block-interleavers were proposed in order to average the channel over each of the information block.

The previous error correcting schemes allow to reduce the TTD and to enhance the error correction performance under low Carrier to Noise ratio (C/N_0) environments. However, those channel coding schemes may be limited in terms of error correction performance over harsh environments such as fading and jamming scenarios. Furthermore, considering that the new generation of commercial receivers are expected to acquire and track the signal under extremely low C/N_0 environments, new co-design structures which enhanced error correction capabilities are required.

In this paper, we exploit the "carousel" nature of the broadcasted navigation message to design a channel coding scheme that can fulfill the previous requirements. This joint design between the navigation message and the error correction scheme is based on the family of nested Root-LDPC (Ortega & Poulliat, 2021) codes, which allows to inherently adapt the channel coding rate depending on the number of received blocks. Then, the demodulation threshold is improved by combining different received blocks which allows a lower channel coding rate at the decoder.

1.1 | Contributions

In this paper, we present the methodology to build channel coding schemes which are jointly designed with the navigation message and which are characterized by the MDS and the full diversity properties as well as the capability to combine different information blocks in order to mimic a lower channel coding rate at the decoder. In order to design the error correcting structures, we start by modeling the message structure acquisition considering a block fading channel with erasure. Thus, the data and the redundant information from the encoder are divided into different information blocks. In this context, two different schemes are proposed and analyzed:

1. The first scheme proposes to use a simple regular Nested Root-LDPC code of rate $R = 1/3$ and to split the information and redundant data in three different blocks. This extends our preceding work by considering a splitting of the navigation message over more information blocks. This simple scheme aims to show that this message structure can bring performance enhancement over the existing propositions. To this end, we verify that the error correction performance only depends on the number of received blocks and that it is independent of the received blocks. Moreover, in this article, in order to improve the error correction performance under fading environments, we include independent block-interleavers (i.e. one per information block) to take into account channel variations smaller than one received block. Note that this interleaving strategy is used to average the channel over each of the received block.

2. Then, we extend the previous scheme to the irregular case by considering Protograph based Nested Root-LDPC structures of rate $R = 1/3$. The proposed family imposes a Protograph structure, which can be optimized in order to enhance the error correction performance under the BP decoding algorithm. Following Ortega & Poulliat (2021), we designed protographs based on the PEXIT-Chart method from Liva & Chiani (2007) which allows to optimize the demodulation threshold of the error correcting scheme. As in the preceding case, we include several block-interleavers in order to average the channel over each received block.

The two error correcting schemes along with a new message structure are simulated and compared to each other. The proposed schemes are also compared to the GPS L1C CED error correcting scheme (GPS-L1C-ICD, 2021), that will be considered as a benchmark system. Moreover, we would like to underline that part of this work was already published by the authors in Ortega et al. (2019).

The paper is organized as follows. Section 2 reviews the requirements for co-designing the message structure and the desired channel coding properties to reduce the time to retrieve the CED. Section 3 presents the error correcting solutions. Their performance are presented and analyzed over the block fading channel in Section 3.4. Then, we present the performance over standard channels such as AWGN, jamming and urban channels in Section 3.5. Conclusions are finally drawn in Section 4.

2 | REVIEW OF THE CO-DESIGN OF MESSAGE OF STRUCTURE AND DESIRED CHANNEL CODING PROPERTIES

Over the past few years, the GNSS community has addressed the issue of designing fast and robust acquisition GNSS signals. Several aspects must be taken under consideration in order to design a new fast acquisition component, however the most important criterion is to provide the lowest $TTFF$ as possible. The $TTFF$ is defined as the time needed by the receiver to calculate the first position fix. This time can be defined as the contribution of different times which depends not only of the navigation message design but also of the receiver hardware quality. Among the different time contributions, the time which represents the major contribution is the time needed to retrieve the CED (Schotsch et al., 2017), denoted as TTD. The navigation message acquisition model which allows to reduce the TTD was first proposed in Ortega et al. (2018a 2020). This model handles a reduction of the TTD under high C/N_0 environments without degrading the performance under low C/N_0 channel conditions. This model assumes a GNSS receiver without stored data (i.e. cold start scenario). Under this scenario, the GNSS receiver can start to acquire the information data broadcasted by any GNSS satellite at any symbol period within the navigation message. If the first acquired symbol corresponds to the first information symbol of the CED, the optimal TTD is achieved, otherwise all the navigation message must be received in order to be able to decode the CED.

Based on the preceding idea, in Ortega et al. (2018a 2020), it is proposed to model the data navigation acquisition model as a block fading channel with block erasures (Figure 1 illustrates a codeword under the block fading channel scenario). We define $t = 1, \cdots, n_c$ as the index of the fading blocks. This model allows to consider the missing navigation data as an erased information block and the received navigation data as recovered data information with different average signal to noise ratios. Thanks to this model, we can find a joint design of the navigation message and the channel coding that allow us to decode the CED even if some part of the navigation message is still missing. Note that as the receiver does not need to receive all the navigation data to decode the CED, the TTD can be reduced. In Ortega et al. (2018a 2020), it is also provided the co-design requirements in order to provide a navigation message structure that reduces the TTD. The proposed structure and the different assumptions and constraints can be summarized as follows:

1. CED and redundant data (from the channel encoder) are divided in several blocks. At the receiver, if any block has not been received, the decoder must consider that block as an erased block.

2. A Cyclic redundancy check (CRC) code has to be included within the CED. This CRC code is used to check the integrity of the CED.

3. The co-design must provide the capability to decode the CED even if some information blocks are missing/erased. However, the error correction performance are limited by the amount of missing information blocks. Therefore, if the CRC detects an error, the receiver can still wait for missing erased blocks in order to enhance the error correcting performance. This flexibility at the receiver is required in order to be able to retrieve the CED under harsh environments.

4. Assuming that the CED and redundant data are part of a codeword, a co-design scheme does not allow the use of entire codeword interleavers. Indeed, this structure enforces to receive the *entire* codeword to decode the CED. Consequently, considering a co-design scheme with an interleaver spanning the entire codeword cannot help to reduce the TTD compared to existing systems.

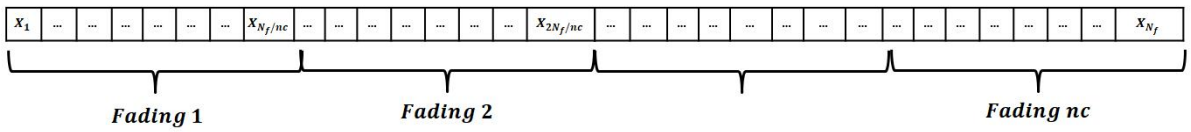

FIGURE 1 Block Fading Message Structure

2.1 | Desired Code Properties

In order to design channel coding schemes suited for the block fading channel with block erasures, three main properties are required:

1. MDS (Maximum Distance Separable) property,
2. Full Diversity,
3. Capability to mimic the channel coding rate (Ortega & Poulliat, 2021).

Let us consider an error correcting scheme, which provides codewords divided in n blocks of equal sizes. We further assume that the CED is embedded into k blocks with $k < n$ of the same size. The MDS property allows to retrieve k data blocks of systematic information from any k error free received blocks. Thanks to this property, we can reduce the TTD under high C/N_0 environments, since with only k error free data blocks, the CED can be retrieved. However, it is possible to find in the literature several references (Boutros et al., 2010; i Fabregas & Caire, 2006; Knopp & Humblet, 2000) where error correcting schemes with MDS property exhibit poor error correction performance over the block fading channel, since they are not able to achieve the *full diversity* of the channel.

Definition 1. An error correcting code C is said to have full diversity over block fading channel if the diversity order is equal to the number of fading blocks n_c. The *diversity* order determines the slope of the error-rate curves as a function of the SNR on a log-log scale for Rayleigh fading distribution:

$$d = -\lim_{\gamma \to \infty} \left(\frac{\log(P_{ew}(\gamma))}{\log(\gamma)} \right), \tag{1}$$

where P_{ew} is the codeword error probability at the decoder output and γ is the average SNR. Then, the P_{ew} of a code with full diversity n_c decreases as $1/\gamma^{n_c}$ at high SNR. Since the error probability of any coding/decoding scheme is lower-bounded by the outage probability P_{out}, the diversity order is upper-bounded by the intrinsic diversity of the channel, which reflects the slope of the outage limit. When maximum diversity is achieved by a code, the coding gain yields a measure of "SNR proximity" to the outage limit. This optimal design yields the optimal code, which is given by the Singleton bound:

$$d \leq 1 + \lfloor n_c(1 - R) \rfloor \tag{2}$$

Codes achieving the Singleton bound are termed MDS. MDS codes are outage-achieving over the (noiseless) block-erasure channel, but may not achieve the outage probability limit on noisy block-fading channels and as a consequence a good coding gain. As a matter of fact, MDS codes are necessary, but not sufficient to approach the outage probability of the channel and it is rather the full diversity property which is the desired and sufficient condition in order to approach the outage probability. Notice from (2) that, in order to find a full diversity code ($d = n_c$), the maximum achievable rate is $R = 1/n_c$. MDS and full diversity properties are achieved by the family of Root-LDPC codes (Boutros et al., 2010) under iterative BP decoding algorithm.

This family of structured codes is characterized by a new check node structure, referred to as rootcheck node, which enables to tolerate more than one erasure bit under BP decoding algorithm. As an example, considering a block fading channel with $n_c = 2$, a rootcheck $\Phi(x_1, x_2, \dots, x_y)$ for a binary element x_1 transmitted on fading α_1 is a checknode where all bits $x_2, \dots, x_y$ are transmitted on fading α_2.

Finally, we search for error correcting structures of rate $1/n$ which are inherently able to adapt the channel coding rate as a function of the number of received data blocks. Thus, we search a code structure where the codeword is divided in n blocks and where the information bits can be decoded over the block fading channel (with $n_c = n$) with a diversity order equal to r, with $r < n$ is the number of received data blocks. Note that in that case, the information data achieves full diversity when $r = n_c$. Moreover, the error correcting structure should provide equal coding gain, independently of the received blocks. Note that in this case, the error correction performance only depends on the number of received blocks. As an illustrated example, let us consider a family of such structured codes with rate $1/3$ over a block fading channel with $n_c = 3$. When only $r = 2$ blocks are received, the information bits should be decoded with a diversity order equal to those decoded by a Root-LDPC code structure of rate $1/2$ over a block fading channel with $n_c = 2$.

3 | PROPOSED ERROR CORRECTING SCHEMES OF RATE 1/3

In this section, we present a regular LDPC code structure with MDS and full diversity properties as well as the capability of combining different information blocks to adapt the channel coding rate (also called nested property). Thanks to those combined properties, the decoder is capable to reduce the TTD and to provide enhanced error correction performance and lower demodulation threshold (Ortega et al., n.d.). Secondly, we extend this coding structure to the irregular case, which improves the previous channel coding structure by optimizing its structure based on a protograph based design approach. Thus, the following schemes will be analyzed:

- Regular Nested Root-LDPC code of rate 1/3,
- Irregular Nested Protograph Root-LDPC code of rate 1/3.

Note that in this paper, for the sake of the presentation and illustration of the proposed message broadcasting strategy, we are only considering the design of error correcting schemes of rate $R = 1/3$. However, as it is shown in Ortega & Poulliat (2021); Ortega et al. (2019), lower coding rate can also be considered by extending the design method given in this paper.

3.1 | Nested Root-LDPC codes of rate 1/3

In this section, we present the family of Nested Root-LDPC codes of rate 1/3 (Ortega et al., 2019). For this family of codes, the considered message structure assumes that the overall message, i.e. the CED and redundant data from the channel encoder, is split over 3 information blocks and it is characterized by the following properties:

- The MDS property, which allows to retrieve the CED from any information block free of errors.
- The full diversity over the block fading channel when the BP algorithm is used. It allows to decode the CED with a diversity order equal to the number of received information blocks.
- Moreover, when the receiver has already received $r = 2$ information blocks, the CED can be decoded with a diversity of order 2. Moreover, independently of the received information block, same coding gain is achieved. This prooerty is referred to as the nested property.

Each systematic codeword (corresponding to the CED information + redudant data) is divided into 3 information blocks, each of them containing some information and redundant data. More precisely, considering a codeword of length $N = 1800$ bits, each information block includes $N/9 = 200$ bits of information data and $2N/9 = 400$ bits of redundant data. Note that since the coding rate is $R = 1/3$, each information block is composed of $N/3 = 600$ bits. The LDPC code base matrix can be described as follows:

$$\boldsymbol{H}_{\beta} = \begin{bmatrix} \boldsymbol{I}_{1,1} & \boldsymbol{0} & \boldsymbol{0} & \boldsymbol{h}_{1,4} & \boldsymbol{h}_{1,5} & \boldsymbol{h}_{1,6} & \boldsymbol{0} & \boldsymbol{0} & \boldsymbol{0} \\ \boldsymbol{I}_{2,2} & \boldsymbol{0} & \boldsymbol{0} & \boldsymbol{0} & \boldsymbol{0} & \boldsymbol{0} & \boldsymbol{h}_{2,7} & \boldsymbol{h}_{2,8} & \boldsymbol{h}_{2,9} \\ \boldsymbol{h}_{3,1} & \boldsymbol{h}_{3,2} & \boldsymbol{h}_{3,3} & \boldsymbol{I}_{3,4} & \boldsymbol{0} & \boldsymbol{0} & \boldsymbol{0} & \boldsymbol{0} & \boldsymbol{0} \\ \boldsymbol{0} & \boldsymbol{0} & \boldsymbol{0} & \boldsymbol{I}_{4,4} & \boldsymbol{0} & \boldsymbol{0} & \boldsymbol{h}_{4,7} & \boldsymbol{h}_{4,8} & \boldsymbol{h}_{4,9} \\ \boldsymbol{h}_{5,1} & \boldsymbol{h}_{5,2} & \boldsymbol{h}_{5,3} & \boldsymbol{0} & \boldsymbol{0} & \boldsymbol{0} & \boldsymbol{I}_{5,7} & \boldsymbol{0} & \boldsymbol{0} \\ \boldsymbol{0} & \boldsymbol{0} & \boldsymbol{0} & \boldsymbol{h}_{6,4} & \boldsymbol{h}_{6,5} & \boldsymbol{h}_{6,6} & \boldsymbol{I}_{6,7} & \boldsymbol{0} & \boldsymbol{0} \end{bmatrix}, \tag{3}$$

where $\boldsymbol{I}_{i,j}$ and $\boldsymbol{0}$ are $N/9 \times N/9$ identity and all-zero matrices respectively. $\boldsymbol{h}_{i,j}$ are submatrices with same Hamming weights per row and column. Moreover, the subindexes i and j represent the row and the column position within the base matrix. Moreover, the base matrix requires the following Hamming weights symmetry $|\boldsymbol{h}_{3,1}| = |\boldsymbol{h}_{6,4}| = |\boldsymbol{h}_{2,7}|$, $|\boldsymbol{h}_{5,1}| = |\boldsymbol{h}_{1,4}| = |\boldsymbol{h}_{4,7}|$, $|\boldsymbol{h}_{3,2}| = |\boldsymbol{h}_{6,5}| = |\boldsymbol{h}_{2,8}|$, $|\boldsymbol{h}_{5,2}| = |\boldsymbol{h}_{1,5}| = |\boldsymbol{h}_{4,8}|$, $|\boldsymbol{h}_{3,3}| = |\boldsymbol{h}_{6,6}| = |\boldsymbol{h}_{2,9}|$, $|\boldsymbol{h}_{5,3}| = |\boldsymbol{h}_{1,6}| = |\boldsymbol{h}_{4,9}|$. Note that $|\cdot|$ represents the Hamming weight. The Hamming weight distribution used for this error correcting structure is the regular structure (4,6), i.e. $|\boldsymbol{h}_{i,j}| = 1$ when $j = \{1, 4, 7\}$, otherwise $|\boldsymbol{h}_{i,j}| = 2$.

3.2 | Navigation message structure adapted to Nested Root-LDPC of rate $1/3$

Following the idea of the navigation message structure presented in Ortega et al. (2018a 2020), the structure of the message is composed of a series of messages with the same structure as the GPS L1C message in GPS-L1C-ICD (2021) (please refers to Figure 2 to check the GPS L1C signal structure and Figure 3 to check the proposed message structure, respectively). Note that each message is split in three different parts. The first part contains 52 bits used to demodulate the Time of Interval (TOI) (GPS-L1C-ICD, 2021). The second part contains the CED and redundant data required to apply an error correcting algorithm at the receiver to demodulate the CED. Finally, the third part (also known as subframe 3) contains 274 bits of additional data and 274 bits of redundant data (called in Figure 2 as "Data" 1 and "Redundant" Data 1). Thus, we have 1800 bits per message. Since the GPS L1C signal is transmitted with a data rate of 100 bits/second, the demodulation of the GPS L1C message is 18 seconds. Note that the difference between the GPS L1C message structure and the proposed message structure is that whereas for GPS L1C message the information contained in the second part (CED and redundant data) is the same for each message, in the proposed navigation message, there are three possible types of messages.

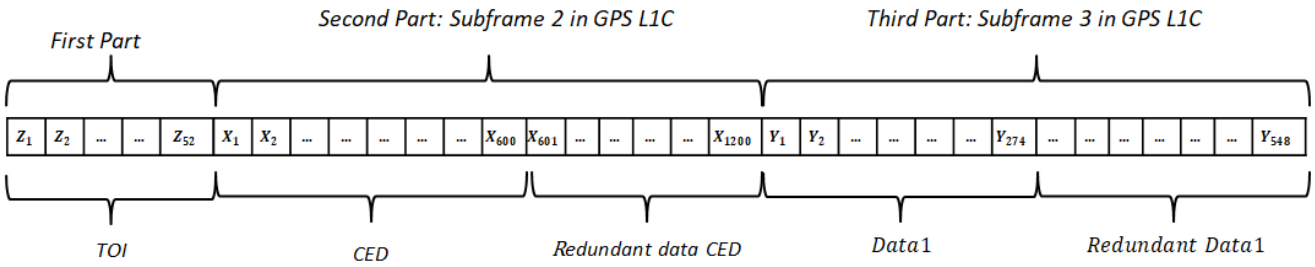

FIGURE 2 GPS L1C navigation message structure.

The detailed structure is given as follows:

- The 1st message sends the first and the second information blocks which contain $2/3$ of the CED (400 bits) and $2/3$ of the redundant data (800 bits). With this data, we are able to retrieve the CED with the same resilience as a Root-LDPC code of rate $1/2$.
- The 2nd message sends the third and the first information blocks which contain $2/3$ of the CED (400 bits) and $2/3$ of the redundant data (800 bits). Again, with this data we are able to retrieve the CED with the same resilience as a Root-LDPC code of rate $1/2$. Moreover, if we have already received the 1st message, we can enhance the resilience of the data since we have already received the precedent 200 bits of CED and the 400 bits of redundant data, equivalent to a channel coding scheme of $1/3$.

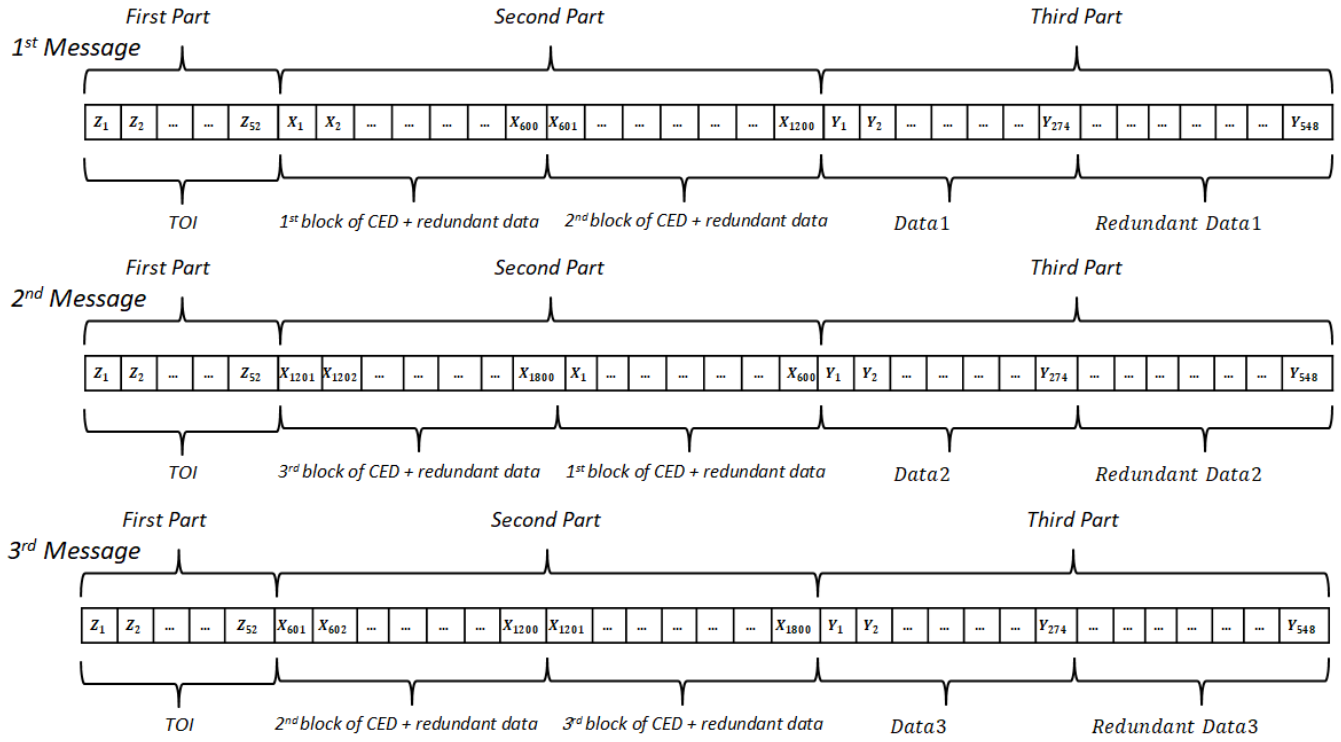

FIGURE 3 Navigation message structure for a Nested Root-LDPC of rate 1/3.

- The 3rd message sends the second and the third information blocks which contain $2/3$ of the CED (400 bits) and $2/3$ of the redundant data (800 bits). Again, with this information we are able to retrieve the CED with the same resilience as a Root-LDPC code of rate $1/2$. Moreover, if we have already received the second message, we can enhance the resilience of the data.

In principle, one might think that sending more information involves higher time to demodulate the CED. However, since the proposed codes are MDS, under good channel conditions it is possible to retrieve the CED when only one information block has been received. Thanks to this fact, the proposed structure can reduce the TTD. Futhermore, we would like to underline that in the GPS L1C structure, one interleaver is used within the second and third part of the message to improve the channel diversity. Note that the use of this type of interleaver enforces that the TTD cannot be reduced. For the proposed navigation message structure, in order to improve the channel diversity over the block fading channel with $n_c > n$, we might include a **block-interleaver** to each of the information block (as it has been proposed for the Root-LDPC codes in Ortega et al. (n.d.)). Note that including a block-interleaver enhance the channel diversity at the receiver without increasing the TTD of the Nested Root-LDPC message structure.

3.3 | Construction of Protograph-based Irregular Nested Root-LDPC codes of rate 1/3

The preceding regular case is of interest to analyze the desired properties of the proposed navigation message structure. However, as the variable node degree is even by construction for the regular case, it does not lead to real practical schemes and encoding and mapping the information bits within the i_k classes becomes an issue. In real implementations, small modifications of the structure are applied in order to obtain encodable structures. However, the properties of these codes may slightly differ from those obtained theoretically for regular codes.

In this section, we investigate on the design of Protograph Nested Root-LDPC codes which enables to design codes that lead to practical solutions with optimized demodulation thresholds when two or three blocks information blocks have been received. Considering the base matrix in equation (3), we adopt the following general protograph representation (Thorpe, 2003)

$$\boldsymbol{H}_B = \begin{bmatrix} 1 & 0 & 0 & * & * & * & 0 & 0 & 0 \\ 1 & 0 & 0 & 0 & 0 & 0 & * & * & * \\ * & * & * & 1 & 0 & 0 & 0 & 0 & 0 \\ 0 & 0 & 0 & 1 & 0 & 0 & * & * & * \\ * & * & * & 0 & 0 & 0 & 1 & 0 & 0 \\ 0 & 0 & 0 & * & * & * & 1 & 0 & 0 \end{bmatrix}, \tag{4}$$

where $* \in \mathbb{N}^*$, $i \in \{1, \cdots, m\}$ and $j \in \{1, \cdots, n\}$, represent possible parallel edges in the proto representation (Thorpe, 2003). Note that if we use the Protograph EXIT (PEXIT) Chart algorithm proposed in Liva & Chiani (2007) to search for coefficients $*$, the retrieved matrix is not necessary symmetrical between the different blocks. As a consequence, the base matrix does not ensure the required Hamming weight symmetrical pattern to fulfill the nested property.

Considering this fact and setting unknown $'*'$ to be coefficient weights $\in (0, 1, 2, 3)$, we apply the optimization procedure proposed in Ortega & Poulliat (2021):

1. We search for the subset of protograph matrices that provide the symmetrical pattern of the base matrix in equation (3).
2. We compute the demodulation threshold over the ergodic channel (i.e. AWGN channel) when only two blocks are received. To do that, we compute the PEXIT chart algorithm with one erased block, i.e. considering that the channel mutual information provided by the erased block is $I_{\alpha_t} = 0$. Note that it is simple to verify (Ortega & Poulliat, 2021) that if the protograph base matrix ensures the symmetrical pattern, the observed demodulation threshold is independent of the received blocks.
3. We compute the demodulation threshold over the ergodic channel when the entire codeword is received (i.e. when the three blocks are received). In this case, we compute the PEXIT chart algorithm considering the ergodic AWGN channel.
4. We proceed to select the protograph structure that minimizes the demodulation thresholds in previous steps. Note that some protograph structures can provide low demodulation thresholds for the second step but high demodulation thresholds for the third step. In this design, we look for the protograph structure that minimizes the demodulation threshold of the second step, considering that the demodulation threshold in the third step is lower that the structure provided in section 3.1 .

By applying the above procedure, we have obtained the following base matrix:

$$H_B = \begin{bmatrix} 1 & 0 & 0 & 1 & 0 & 3 & 0 & 0 & 0 \\ 1 & 0 & 0 & 0 & 0 & 0 & 0 & 2 & 2 \\ 0 & 2 & 2 & 1 & 0 & 0 & 0 & 0 & 0 \\ 0 & 0 & 0 & 1 & 0 & 0 & 1 & 0 & 3 \\ 1 & 0 & 3 & 0 & 0 & 0 & 1 & 0 & 0 \\ 0 & 0 & 0 & 0 & 2 & 2 & 1 & 0 & 0 \end{bmatrix}. \tag{5}$$

As previously mentioned, we propose to add a **block-interleaver** associated to each of the information block in order to enhance the diversity of the channel. Regarding the encoding, most of existing strategies for encoding LDPC codes can be applied. In particular, as we are mostly dealing with protograph LDPC codes enabling quasi-cyclic structures, existing efficient encoding methods are available in Li et al. (2006).

3.4 | Evaluating the Nested Root-LDPC family properties over the block Rayleigh fading channel

In this section, we analyze the performance of the two proposed Nested Root-LDPC codes of rate $R = 1/3$ over the block fading channel. We also analyze the performance of these families over the block fading channel considering that one block-interleaver is included for each sent block.

In Figure 4 , the CED error rate (CEDER) of the regular Nested Root-LDPC family of rate $R = 1/3$ for a block Rayleigh fading channel with $n_c = 3$ is illustrated. Moreover, this family of codes are also evaluated when one interleaver structure per block is include in the error correcting structure. Finally, the outage probability P_{out} (Boutros et al., 2010) for a Binary Phase Shift Keying (BPSK) input with $R = 1/3$ and block fading channel with $n_c = 3$ is also included. Note from Figure 4 that both structures achieve the full diversity property since the CEDERs have the same slope as the outage probability curve. We also realize that the Protograph structure presents better error correction performance due to its higher coding gain (Ortega &

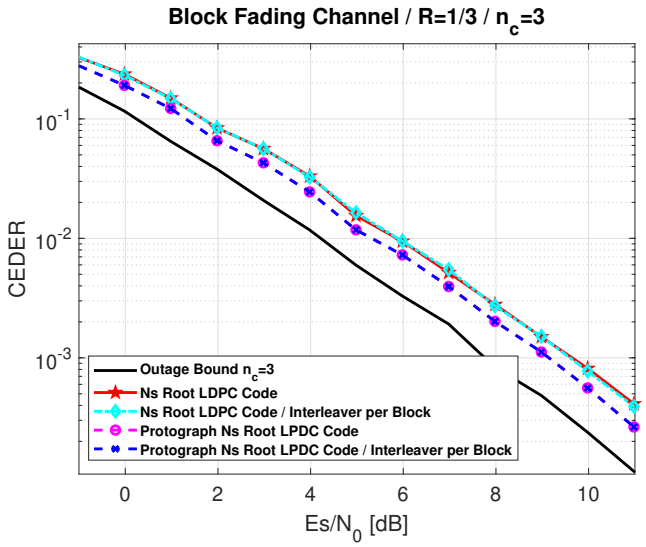

FIGURE 4 CEDER for Nested Root-LDPC structures with $R = 1/3$ and $n_c = 3$.

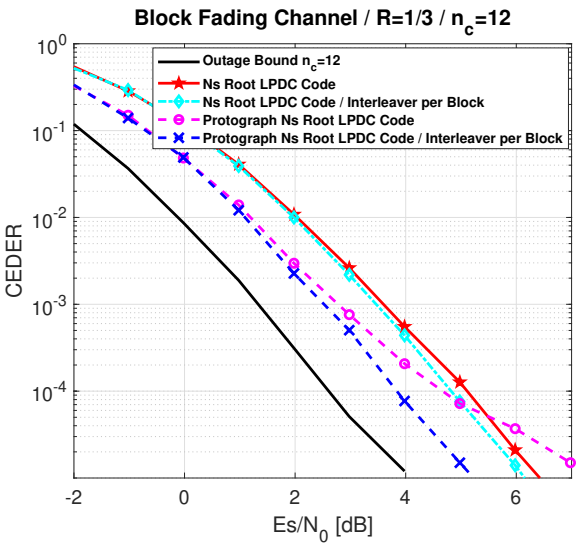

FIGURE 5 CEDER for Nested Root-LDPC structures with $R = 1/3$ and $n_c = 12$.

Poulliat, 2021) (the CEDER performance are closer to the outage probability curve). Finally, we note that the interleaver per block does not enhance the error correcting performance since full diversity has been already guaranteed.

In Figure 5 , the previous error correcting structures are evaluated in terms of CEDER for a block Rayleigh fading channel with $n_c = 12$. In this Figure, it is also included the outage probability P_{out} for a BPSK input with $R = 1/3$ and block Rayleigh fading channel with $n_c = 12$, i.e. one information block can now experience several block fading attenuations. As expected, we note from this Figure that full diversity is not achieved. However, adding one interleaver per block helps to increase the channel diversity and consequently to improve the error correcting performance. Again, the Protograph structure presents better error correction performance due to its higher coding gain.

In Figure 6 , we illustrate the CEDER of the regular Nested Root-LDPC codes and the Protograph-based irregular Nested Root-LDPC of rate $R = 1/3$ for a block fading channel with $n_c = 3$, considering that only two information blocks are received. We have considered the following possible scenarios: i) the 1st and the 2nd information blocks are received; ii) the 1st and the 3rd information blocks are received and iii) the 2nd and the 3rd information blocks are received. Moreover, we have also included the CEDER of a regular (3,6) Root-LDPC code (Boutros et al., 2010) of rate $R = 1/2$ and the outage probability curve for a code of rate $R = 1/2$ for a block fading channel with $n_c = 2$. Note from this Figure that both structures achieve a diversity equal to 2, independently of which blocks have been received. Moreover, the error correction performance are independently of the received blocks. Again, we can notice that the Protograph structure provides better error correction performance due to its higher coding gain.

In Figure 7 , we illustrate the CEDER of the Protograph Nested Root codes of rate $R = 1/3$ for a block fading channel with $n_c = 12$, considering that only two of the information blocks are received. Again, the following scenarios are considered: i) the 1st and the 2nd information blocks are received; ii) the 1st and the 3rd information blocks are received and iii) the 2nd and the 3rd information blocks are received. Moreover, we plot the curves corresponding to the same code structure when two information block are received and one block-interleaver is added per block. Finally, we plot the outage probability curve when only two blocks are received. Note from this Figure that the block-interleaver helps to increase the channel diversity, obtaining almost the maximum diversity and consequently enhancing error correcting performance with respect to the code structure without one block-interleaver per block.

3.5 | Evaluation for standard scenarios

In order to compare the performance of the error correcting solutions, in this subsection the CEDER is evaluated over AWGN, pulsed jamming and urban channels.

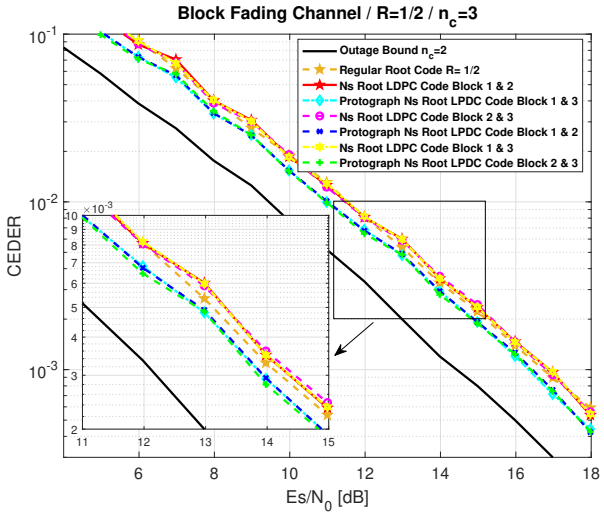

FIGURE 6 CEDER for Nested Root structures with $R = 1/3$ and $n_c = 3$ when two fading blocks are received.

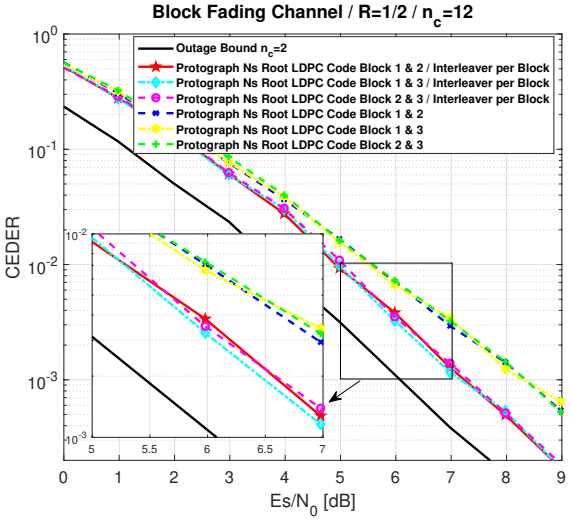

FIGURE 7 CEDER for Nested Root structures with $R = 1/3$ and $n_c = 12$ when two fading blocks are received.

3.5.1 | Results over AWGN channel

We first consider an AWGN channel. The AWGN channel is the model used to estimate the background noise on the open-sky transmission channel. This model does not include fadings or interferences coming from other sources. We represent the transmitted message as a binary vector $\mathbf{u} = [u_1, \cdots, u_K]$ of K bits. This message is encoded into a codeword $\mathbf{c} = [c_1, \cdots, c_N]$ of length $N > K$ and mapped to BPSK symbols $x_n = \mu(c_n) \in \{-1, 1\}$, where n represents the symbol time index and $\mu(c) = 1 - 2c$.. The transmission channel is modeled as a binary-input AWGN noise channel with variance $\sigma^2 = \frac{N_0 \cdot B}{2}$ and B the received frequency band. Then, the received symbol sequence y_n is modeled as:

$$y_n = x_n + w_n, \tag{6}$$

where $w_n \sim \mathcal{N}(0, \sigma^2)$. Note that, for this model, complete channel state information (CSI) is considered at the receiver, i.e. σ^2 is considered as known.

When one information block has been received, thanks to the MDS property, we can retrieve the information data (CED) when the C/N_0 is high. As a consequence, we reduce the TTD when compared with the structure provided by the GPS L1C subframe 2, since we do not have to wait to receive all the data. This is illustrated in Figure 8 , where the TTD values for a AWGN scenario with $C/N_0 = 45$ dBHz are provided. In order to obtain the TTD values, we need to define the Probability Density Function (PDF) $f(t)$ of the TTD. Then, the time to retrieve the CED can be obtained from the Cumulative Distribution Function (CDF) defined as follows:

$$CDF(TTD) = \int_{-\infty}^{TTD} f(t)dt = x \tag{7}$$

where x describes the percentage of confidence needed in order to represent the time needed by the receiver to retrieve CED. For simulations, we evaluate 100.000 times the duration needed by one receiver to obtain the error free CED. As expected, the first epoch (first synchronized bit) can arrive at any time. Following the CED structure of GPS L1C subframe 2 and the navigation message structure defined in Section 3.2, each message represents 1800 bits, therefore in order to initialize the first epoch value for each of the 100.000 simulations, an uniform distribution with values between 1 and 1800 is used. Each of the values represents a possible first synchronized bit. Simulation results in Figure 8 show a reduction of more than 30% of TTD for at least 66% of the time compared to the current GPS L1C signal and a reduction of 50% of TTD for at least 30% of the time in case of the Nested Root-LDPC scheme (with a $C/N_0 = 45$ dBHz channel conditions).The TTD reduction can be explained due to the fact that when one block of information is received correctly, the demodulation algorithm is capable to retrieve the 400 missing CED bits. In other words, when 600 bits from the navigation message are received, there is a non-zero probability that

they correspond to the bits of a block of information (200 CED bits and 400 redundancy bits) and therefore the demodulation algorithm can retrieve the 400 missing CED bits. Note that having received $600 + x$ bits with high enough C/N_0 increases the probability to retrieve at least one block of information and it enables to retrieve the missing CED bits. In Figure 8 , TTD curves when the $C/N_0 = 35$ dBHz (standard operating point for the GPS L1C data signal as it is shown in Das et al. (n.d.); Medina et al. (2020)) are illustrated. Once again, it can be shown a reduction of the TTD for the coding structures that use Nested Root-LDPC codes even if the channel conditions are degraded. This is due to the fact that once more than one block of information has been received, the data demodulation algorithm can either be used to retrieve the missing CED or to correct possible errors.

Regarding the error correction capabilities of the proposed scheme, CEDER performance of Nested Root-LDPC codes are reported in Figure 9 when two information blocks have been received. As it can be seen, we can retrieve the information data (CED) with an error correction performance almost similar to the GPS L1C subframe 2 structure. We just observe a small gap of 0.55 dBHz for an error probability of 10^{-2}. When three information blocks have been received, the error correcting performance are better than that of the structure provided by the GPS L1C subframe 2 at 1.2 dBHz for an error probability of 10^{-2}. As a consequence, the receiver devices can operate in the range of $C/N_0 = 22 - 24$ dBHz (low sensitivity devices). Moreover, we underline that Protograph Nested Root-LDPC codes of rate $1/3$ improve the error correction performances by 0.25 dB for an error probability of 10^{-2} when 2 blocks have been received. Moreover, when the entire codeword has been received, the Protograph version of the Nested Root-LDPC of rate 1/3 improves by 0.7 dB for an error probability of 10^{-2}. Note that the GPS L1C system is not capable to operate in this range (For $C/N_0 \leq 23$ dBHz, the TTD is ∞) as it is illustrated in Figure 10 . In this Figure, it can be also observed a higher TTD for the Nested Root-LDPC codes structures since channel conditions have been degraded. However, these structures are capable to retrieve a correct CED over the time since they are more resilient due to the fact that they are able to used extra information (3 information blocks) to demodulate the CED. Finally, in Figure 11 , we compare the CEDER curves corresponding to the case of one single received block with respect to 2 or 3 received blocks of information for the Nested Root-LDPC codes. From this Figure, one can verify that when 1 block of information is received with a C/N_0 of 35 dBHz, the CEDER is of the order of 10^{-2}. Then, in the particular example illustrated in Figure 8 with $C/N_0 = 45$ dBHz and $C/N_0 = 35$ dBHz, the proposed navigation structure is expected to have almost no failure in the data demodulation. This fact justifies how the TTD can be reduced significantly when using Nested Root-LDPC codes under standard open-sky channel conditions, i.e, C/N_0 in the range of $35 - 45$ dBHz.

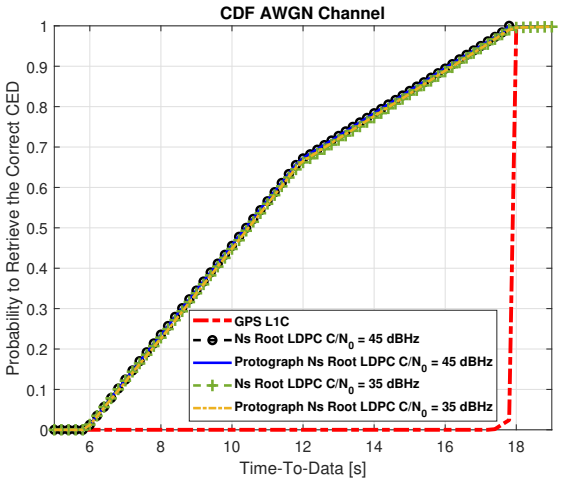

FIGURE 8 CDF of the Nested Root-LDPC codes over AWGN channel with $C/N_0 = 45$ dBHz and $C/N_0 = 35$ dBHz.

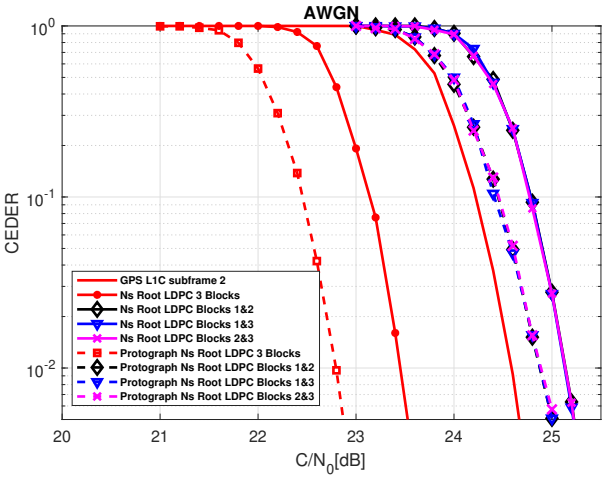

FIGURE 9 CDF of the Nested Root-LDPC codes over AWGN channel with $C/N_0 = 30$ dBHz.

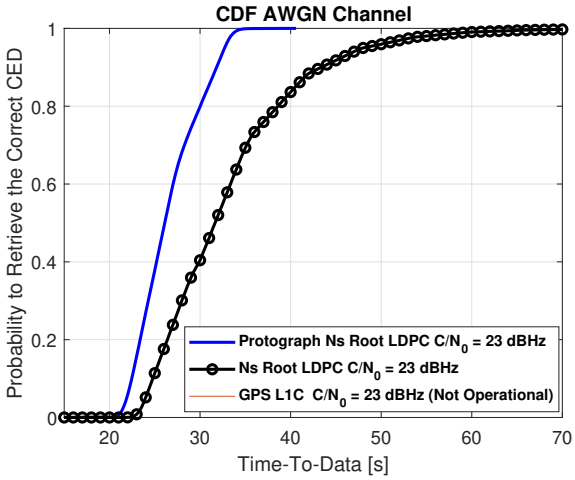

FIGURE 10 CDF of the Nested Root-LDPC codes over AWGN channel with $C/N_0 = 23$ dBHz.

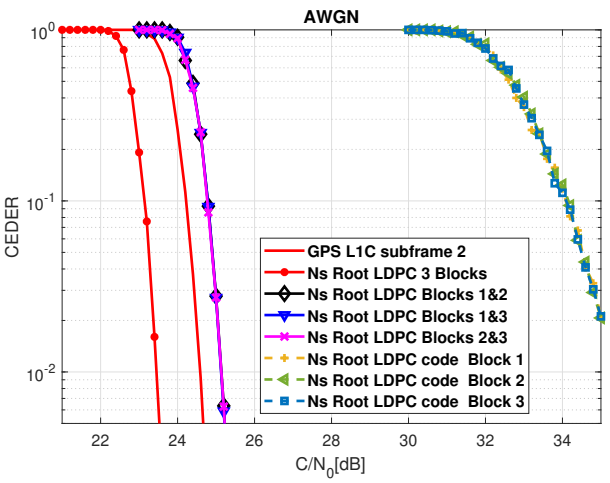

FIGURE 11 CEDER over AWGN channel of a Nested Root-LDPC code of rate $R = 1/3$ when 1, 2 or 3 blocks are received.

3.5.2 | Results for pulsed jamming channel

In this section, we evaluate the results considering a pulsed jamming channel model. This channel considers that a jammer device is broadcasting a Gaussian interference which disrupts some percentage P of the codeword symbols. We can model the channel scenario as follows:

We represent the transmitted message as a binary vector $\mathbf{u} = [u_1, \cdots, u_K]$ of K bits. This message is encoded into a codeword $\mathbf{c} = [c_1, \cdots, c_N]$ of length $N > K$ and mapped to BPSK symbols $x_n = \mu(c_n) \in \{-1, 1\}$.The transmission channel is modeled with an AWGN with instantaneous noise variance σ^2. Moreover, some percentage P of transmitted symbol is disrupted by an extra AWGN with instantaneous noise variance σ_I^2. Then, the received symbol sequence is modeled as:

$$y_n = \begin{cases} x_n + w_n \in \mathbb{R}, & n \in \mathbb{Q}, \\ x_n + w_n + I_n \in \mathbb{R}, & n \in \mathbb{S}, \end{cases} \tag{8}$$

where $w_n \sim \mathcal{N}(0, \sigma^2)$ and $I_n \sim \mathcal{N}(0, \sigma_I^2)$ are the statistical models for the noise and jamming. $\mathbb{Q}$ is the set of bits not affected by the jamming noise and $\mathbb{S}$ is the set of bits disrupted with the jamming. We also have that $\frac{|\mathbb{S}|}{|\mathbb{Q}|+|\mathbb{S}|} = P$, $|.|$ denotes the cardinality of the corresponding ensemble. Finally, the CSI is considered at the receiver, i.e. σ^2 and σ_I^2 are considered known.

In the following simulation, P is fixed to 0.1 and the interference power $P_{int} = 12$dB. In Figure 12 , the CEDER results are provided for the proposed Nested Root-LDPC code and Protograph Nested LDPC code of rate $R = 1/3$. Considering the Nested Root-LDPC structure, if two information blocks have been received, we can retrieve the CED with an error correction performance almost similar to the GPS L1C subframe 2 structure. A gap of 0.75 dBHz for an error probability of 10^{-2} is observed. This gap is reduced to 0.25 dBHz for an error probability of 10^{-2} when considering the Protograph Nested Root-LDPC structure. When three information blocks have been received (red dashed curve), the error correcting performance provided by the regular Nested Root-LDPC code are better than the structure provided by the GPS L1C subframe 2 by almost 1.6 dBHz for an error probability of 10^{-2}. This enhancement of the error correction performance is improved to 3.1 dBHz for an error probability of 10^{-2} when using the Protograph-based irregular Nested Root-LDPC code structure. Simulation results (we have evaluated 100.000 times the duration needed by one receiver to obtain the error free CED) in Figure 13 show a reduction of more than 30% of TTD for at least 66% of the time compared to the current GPS L1C signal and a reduction of 50% of TTD for at least 30% of the time in case of the Nested Root-LDPC scheme (with a $C/N_0 = 45$ dBHz channel conditions). Note that this TTD reduction can be explained by the fact that when 1 block of information is correctly received, the data demodulation algorithm is capable to retrieve the 400 missing CED bits. This performance are degraded when $C/N_0 = 40$ dBHz, but we can still observe a TTD reduction with respect to the GPS L1C system. In addition, we would like to underline that the GPS L1C system is not capable to operate in ranges with $C/N_0 \leq 24$ dBHz as it is illustrated in Figure 12 , i.e. the TTDs for those scenarios are equal to ∞. Finally, in Figure 13 we have also plotted the TTD for the Nested Root-LDPC structure for a $C/N_0 = 24$ dBHz. Note

that, even if there is an increment of the TTD (due to the channel conditions degradation) these structures are able to retrieve a correct CED over the time since they are more resilient due to the fact that they can benefit from extra information to demodulate the CED.

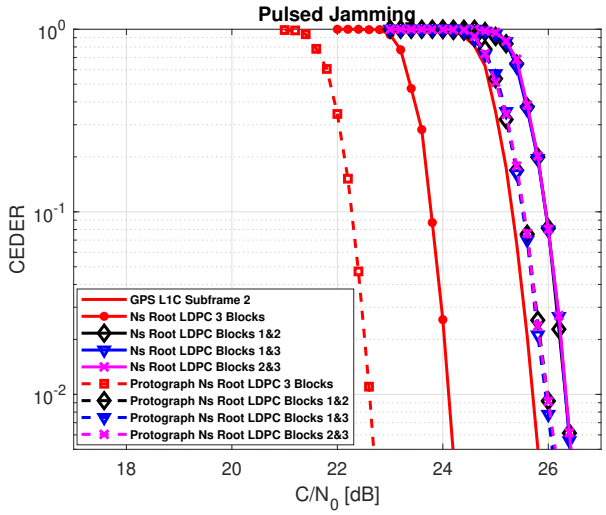

FIGURE 12 CEDER over the pulsed jamming channel with $P = 0.1$ and $P_{int} = 12dB$ for the Nested Root LPDC code and for the Protograph Nested Root LPDC code of rate $R = 1/3$.

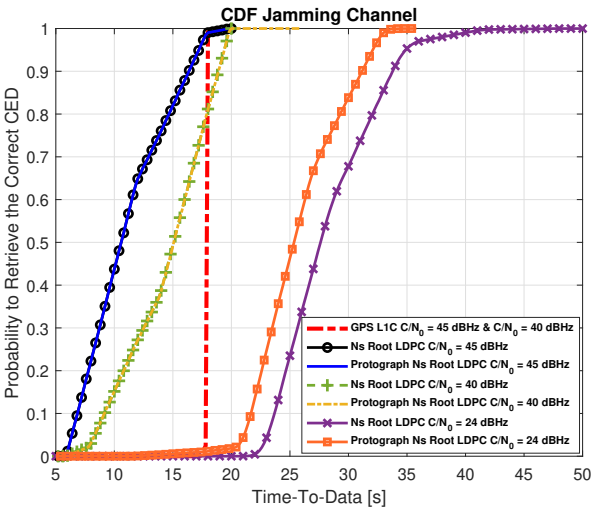

FIGURE 13 CDF of the Nested Root-LDPC codes over the pulsed jamming channel with $P = 0.1$ and $P_{int} = 12dB$ for $C/N_0 = 45$ dBHz, $C/N_0 = 40$ dBHz and $C/N_0 = 24$ dBHz.

3.5.3 | Results for urban channel

To model the urban environment, we have used a 2-state Prieto model (Prieto-Cerdeira et al., 2010) for a vehicle speed of 40 km/h and an elevation angle of 40 degrees. This model considers the fading gain, denoted as h_n. We represent the transmitted message as a binary vector $\mathbf{u} = [u_1, \cdots, u_K]$ of K bits. Using a binary error correcting code of rate $R = K/N$, this message is then encoded into a binary codeword $\mathbf{c} = [c_1, \cdots, c_N]$ of length $N > K$ and mapped to binary phase shift keying (BPSK) symbols $x_n = \mu(c_n) = 1 - 2.c_n \in \{-1, 1\}$, $\forall n = 1 \cdots N$. Modeling the transmission channel as an uncorrelated fading channel with additional real-valued additive white Gaussian noise (AWGN) with noise variance σ^2, the received symbol sequence is then given by:

$$y_n = h_n \cdot x_n + w_n \in \mathbb{R}, \quad n = \{1, \ldots, N\}, \tag{9}$$

where both w_n and h_n are identically and independently distributed (i.i.d.) random variables such that $w_n \sim \mathcal{N}(0, \sigma^2)$ and $h_n \sim p(h)$ respectively. $p(h)$ is defined following the 2-state Prieto model in Prieto-Cerdeira et al. (2010).

In Figure 14 , the results for a regular Nested Root-LDPC code of rate 1/3 are given. The values h_n and σ^2 are considered known at the receiver. Considering the Nested Root-LDPC code, when two information blocks have been received, we can retrieve the information data (CED) with an error correction performance almost similar to the GPS L1C subframe 2 structure. This error correction performance is similar to the GPS L1C subframe 2. With Nested Root-LDPC codes and with three received information blocks, the error correcting performance are better than the structure provided by the GPS L1C subframe 2 by almost 2.5 dBHz for an error probability of 10^{-2}. The error correction capabilites are improved to 3.2 dBHz for an error probability of 10^{-2} when using the Protograph-based irregular Nested Root-LDPC structure. Simulation results (we have evaluated 100.000 times the duration needed by the receiver to obtain the error free CED) in Figure 15 show a reduction of the TTD for at least 80% of the time compared to the TTD of the GPS L1C signal structure when Nested Root-LDPC schemes are used (when the $C/N_0 = \{40, 45\}$ dBHz). Note that the reduction of the TTD can be explained since when more than 1 block of information is received, the data demodulation algorithm can be computed to try to retrieve the 400 missing CED bits. However, unlike

running the demodulation algorithm on the AWGN channel with high C/N_0, when the data is received over the LMS channel, it is possible that it is required more than one block of information even if the C/N_0 is high. This is due to the fact that the LMS channel is a not ergodic channel and fadings events can reduce the instanteanous SNR for a particular set of received symbols. Given the navigation structure presented in Figure 15 , note that if two blocks of information are required to retrieve the CED without error, around 20% of the time, the TTD of the proposed structure is higher than the TTD of the GPS L1C system. This particular case may occur if the receiver starts receiving data at the end of the first information block. Once the second block is received, it is likely that due to the nature of the LMS channel the demodulation algorithm is not capable to correct the errors and it will be necessary to wait for the reception of the third block of information, yielding to higher TTD with respect to the GPS L1C structure. A possible solution to avoid exceeding the TTD of the GPS system is to enforce the data demodulation once 18 seconds of message have been received. These TTD curves for this paticular structure have also been included in Figure 15 when the $C/N_0 = \{40, 45\}$ dBHz. Note that under this particular scenario, the TTD of the proposed scheme never exceeds that of the GPS L1C system.

Finally, we underline that thanks to the fact that these error correcting schemes reduce drastically the demodulation threshold without increasing the TTD, the data can be demodulated in new system operations points (i.e. allowing both (i) the data demodulation in scenarios where standard channel coding families cannot, and (ii) a reduction of the TTD in harsh environments). Note that the demodulation performance can be improved by constructing Nested Root-LDPC families with lower rate. However, the data demodulation through channel decoder using a lower rate implies an increase of the receiver complexity. The complexity/performance trade-off is out of scope of this paper.

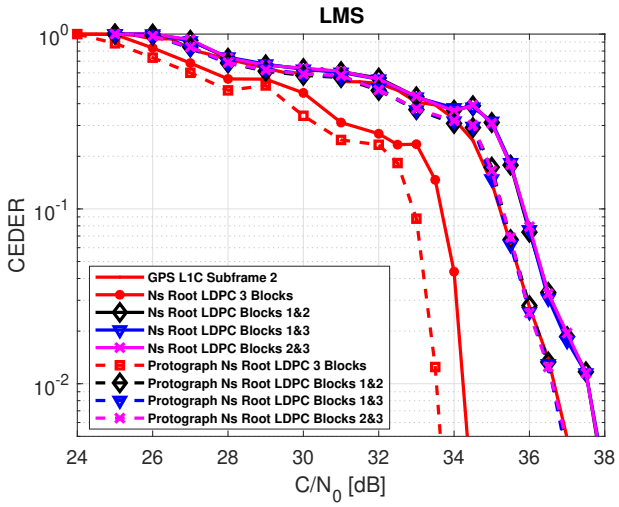

FIGURE 14 CEDER over urban channel of the Nested Root LPDC code and the Protograph Nested Root LPDC code of rate $R = 1/3$.

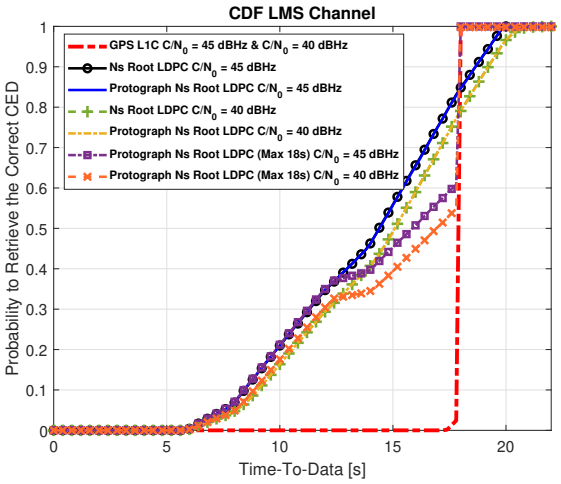

FIGURE 15 CDF of the Nested Root-LDPC codes over urban channel with $C/N_0 = 45$ dBHz and $C/N_0 = 40$ dBHz.

3.5.4 | Effect of the CED size

Since these codes could be applied to any new GNSS signal, in this Section, we compare the error correction performance of the Nested Root-LDPC codes for two different size of the CED. Thus, in Figure 16 , we illustrate the CEDER for a Nested Root-LDPC code of rate $R = 1/3$ when considering a CED size of $600bits$ (i.e. the CED size of the GPS L1C) and a reduced version of the Galileo CED (Anghileri et al., 2012). This reduced version of the CED is intended to be used in future releases of Galileo (Paonni & Bavaro, 2013). The CED information block has 250 bits. Note that reducing the size of the data has a direct impact of the error correcting performance (Richardson et al., 2001). Then, considering the AWGN channel, when only one block is received, lower CED size results in better CEDER. On the other hand, when two or three information blocks are received, lower CED size results in worse CEDER.

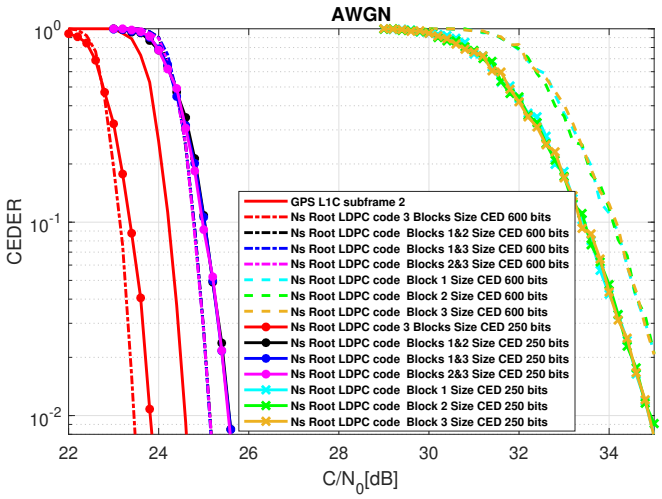

FIGURE 16 CEDER over AWGN channel with two different CED sizes. Nested Root-LDPC code of rate $R = 1/3$ is used as a channel coding scheme.

4 | CONCLUSION

In this paper, we provide the methodology to design error correcting schemes for GNSS systems which are capable to provide MDS and full diversity properties as well as the capability to provide inherent rate adaptation depending on the number of received information blocks, referred to as nested code property. The first property allows the receiver to reduce the TTD in good environments, since with k information blocks we can retrieve the CED. Moreover, thanks to the full diversity property and the nested code property, an enhancement in the error correction performance and in the data demodulation threshold are achievable. Thanks to the improvement of the data demodulation, these structures provide a reduction of the TTD under harsh environments such as low carrier to noise ratio environments, urban environments and pulsed jamming environments. The proposed error correcting structures are then compared with the GPS L1C subframe 2. Simulations show a significant improvement of the error correction performance when three information blocks are received:

- Under AWGN environment when three information blocks are received, an enhancement of the error correction performance of 1.2 and 1.9 dBHz is achieved when using regular Nested Root-LDPC codes and Protograph-based irregular Nested Root-LDPC codes, respectively. Moreover, simulation results show a reduction of more than 30% of TTD for at least 66% of the time compared to the current GPS L1C signal and a reduction of 50% of TTD for at least 30% of the time in case of the Nested Root-LDPC scheme for standard channel conditions, i.e. the C/N_0 in the range of 35 to 45 dBHz). Finally, it is shown that in contrast to the GPS L1C structure, the proposed message structure can be operational in range of $C/N_0 = 22 - 24$ dBHz.

- Under pulsed jamming environment when three information blocks are received, an enhancement of the error correction performance of 1.6 and 3.1 dBHz is achieved when using regular Nested Root-LDPC codes and Protograph-based irregular Nested Root-LDPC codes, respectively. Moreover, simulation results show a reduction of more than 30% of TTD for at least 66% of the time compared to the current GPS L1C signal and a reduction of 50% of TTD for at least 30% of the time when $C/N_0 = 45$ dBHz. In addition, when the channel conditions are degraded, the proposed channel structure is shown to reduce the TTD and to improve the operational range.

- Under urban environment when three information blocks are retrieved, an enhancement of the error correction performance of 2.5/3.2 dBHz are achieved when using regular Nested Root-LDPC codes and irregular Protograph Nested Root-LDPC codes, respectively. Moreover, simulation results show a reduction of TTD for at least 80% of the time compared to the current GPS L1C signal when $C/N_0 = \{40, 45\}$ dBHz. For the other 20% of the cases, the GPS L1C structure obtains a lower TTD than the proposed structure. In order to improve the TTD time, the message can be forced to be demodulated once 18 seconds have been received. Under this configuration, the TTD from the Nested-Root LDPC structure is always lower or equal to the TTD of the GPS L1C system.

ACKNOWLEDGMENT

Part of this work has been presented earlier at the ION GNSS+ 2019 conference (Ortega et al., 2019). This work is part of the PhD dissertation (Ortega, 2019).

CONFLICT OF INTEREST

The authors declare no potential conflict of interests.

References

Anghileri, M., Paonni, M., Gkougkas, E., & Eissfeller, B. (2012). Reduced navigation data for a fast first fix. In *2012 6th esa workshop on satellite navigation technologies (navitec 2012) & european workshop on gnss signals and signal processing* (p. 1-7). https://10.1109/NAVITEC.2012.6423105

Biglieri, E., Proakis, J., & s. Shamai. (1998). Fading channels: Information-theoretic and communications aspects. *IEEE Transactions on Information Theory*, *44*(6), 2619–2692. https://10.1109/18.720551

Blaum, M., & Roth, R. (1999). On lowest density mds codes. *IEEE Transactions on Information Theory*, *45*(1), 46-59. https://10.1109/18.746771

Boutros, J., i Fàbregas, A. G., Biglieri, E., & Zémor, G. (2010). Low-density parity-check codes for nonergodic block-fading channels. *IEEE Transactions on Information Theory*, *56*(9), 4286-4300. https://10.1109/TIT.2010.2053890

Das, P., Ortega, L., Vilà-Valls, J., Vincent, F., Chaumette, E., & Davain, L. (n.d.). Performance limits of gnss code-based precise positioning: Gps, galileo & meta-signals.

Fang, Y., Bi, G., & Guan, Y. (2014). Design and analysis of root-protograph ldpc codes for non-ergodic block-fading channels. *IEEE Transactions on Wireless Communications*, *14*(2), 738–749. https://10.1109/TWC.2014.2359221

Galileo-ICD. (2016). *Galileo - open service - signal in space interface control document (os sis icd v1.3)* (Tech. Rep.). European Union. Retrieved from `https://www.gsc-europa.eu/sites/default/files/sites/all/files/Galileo_OS_SIS_ICD_v2.0.pdf`

GPS-L1C-ICD. (2021). *Interface specification is-gps-800 navstar gps space segment/ usersegment l1c interface* (Tech. Rep.). Retrieved from `https://www.gps.gov/technical/icwg/IS-GPS-800G.pdf`

i Fabregas, A. G., & Caire, G. (2006). Coded modulation in the block-fading channel: Coding theorems and code construction. *IEEE Transactions on Information Theory*, *52*(1), 91–114. https://10.1109/TIT.2005.860414

Knopp, R., & Humblet, P. (2000). On coding for block fading channels. *IEEE Transactions on Information Theory*, *46*(1), 189–205. https://10.1109/18.817517

Li, Y., & Salehi, M. (2010). Quasi-cyclic ldpc code design for block-fading channels. 44th Annual Conference on Information Sciences and Systems (CISS). https://10.1109/CISS.2010.5464729

Li, Z., Chen, L., L.Zeng, Lin, S., & Fong, W. H. (2006). Efficient encoding of quasi-cyclic low-density parity-check codes. *IEEE Transactions on Communications*, *54*(1), 71-81. https://10.1109/TCOMM.2005.861667

Liva, G., & Chiani, M. (2007). Protograph ldpc codes design based on exit analysis. In (p. 3250-3254). IEEE GLOBECOM. https://10.1109/GLOCOM.2007.616

Medina, D., Ortega, L., Vilà-Valls, J., Closas, P., Vincent, F., & Chaumette, E. (2020, Jun). A New Compact CRB for Delay, Doppler and Phase Estimation - Application to GNSS SPP & RTK Performance Characterization. *IET Radar, Sonar & Navigation*. 10.1049/iet-rsn.2020.0168

Ortega, L. (2019). *Signal optimization for galileo evolution*. PhD dissertation. Retrieved from `https://oatao.univ-toulouse.fr/26975/`

Ortega, L., & Poulliat, C. (2021). On nested property of root-ldpc codes. *IEEE Wireless Communications Letters*, *10*(5), 1005-1009. https://10.1109/LWC.2021.3054414

Ortega, L., Poulliat, C., Boucheret, M., Aubault, M., & Al-Bitar, H. (n.d.). Advanced co-design of message structure and channel coding scheme to reduce the time to CED and to improve the resilience for a Galileo 2nd Generation new signal. ESA Workshop on Satellite Navigation Technologies and European Workshop on GNSS Signals and Signal Processing

(NAVITEC 2018), Noordwijk, The Netherlands, 05/12/18-07/12/18. Retrieved from https://oatao.univ-toulouse.fr/22526/

Ortega, L., Poulliat, C., Boucheret, M., Aubault, M., & Al-Bitar, H. (2018a). Co-design of message structure and channel coding scheme to reduce the time to ced and to improve the resilience for a galileo 2nd generation new signal. In (p. 4064-4078). ION GNSS+, Miami, Florida, USA. https://10.33012/2018.15878

Ortega, L., Poulliat, C., Boucheret, M., Aubault, M., & Al-Bitar, H. (2018b). New solutions to reduce the time-to-ced and to improve the ced robustness of the galileo i/nav message. In (p. 1399-1408). ION Position Location And Navigation Symposium, Monterey, California, USA. https://10.1109/PLANS.2018.8373532

Ortega, L., Poulliat, C., Boucheret, M., Aubault, M., & Al-Bitar, H. (2019). Optimal Channel Coding Structures for Fast Acquisition Signals in Harsh Environment Conditions. . https://10.33012/2019.17113

Ortega, L., Poulliat, C., Boucheret, M., Aubault, M., & Al-Bitar, H. (2020). Optimizing the co-design of message structure and channel coding to reduce the ttd for a galileo 2nd generation signal. *NAVIGATION*, *67*(3), 471-492. https://doi.org/10.1002/navi.382

Paonni, M., & Bavaro, M. (2013, September). On the design of a gnss acquisition aiding signal. In (p. 1445-1456). ION GNSS+, Nashville, TN, USA. Retrieved from https://www.ion.org/publications/abstract.cfm?articleID=11330

Prieto-Cerdeira, R., Perez-Fontan, F., Burzigotti, P., Bolea-Alamañ, A., & Sanchez-Lago, I. (2010). Versatile two-state land mobile satellite channel model with first application to dvb-sh analysis. *International Journal of Satellite Communications and Networking*, *28*(5-6), 291-315. https://doi.org/10.1002/sat.964

Richardson, T., Shokrollahi, M., & Urbanke, R. (2001). Design of capacity-approaching irregular low-density parity-check codes. *IEEE Transactions on Information Theory*, *47*(2), 619-637. https://10.1109/18.910578

Richardson, T., & Urbanke, R. (2002). Multi-edge type ldpc codes. Workshop honoring Prof. Bob McEliece on his 60th birthday, California Institute of Technology, Pasadena, California. https://10.1.1.106.7310

Roudier, M. (2015). *Analysis and Improvement of GNSS Navigation Message Demodulation Performance in Urban Environments*. PhD dissertation. Retrieved from https://oatao.univ-toulouse.fr/13649/

Ryan, W., & Lin, S. (2009). *Channel codes: Classical and modern*. Cambridge University Press. Retrieved from https://books.google.fr/books?id=0gwqxBU_t-QC

Schotsch, B., Anghileri, M., Burger, T., & Ouedraogo, M. (2017). Joint time-to-ced reduction and improvement of ced robustness in the galileo i/nav message. In (p. 1544-1558). ION GNSS+, Portland, Oregon, USA. https://doi.org/10.33012/2017.15374

ten Brink, S., Kramer, G., & Ashikhmin, A. (2004). Design of low-density parity-check codes for modulation and detection. *IEEE Transactions on Communications*, *52*(4), 670-678. https://10.1109/TCOMM.2004.826370

Teunissen, P., & Montenbruck, O. (2017). *Handbook of global navigation satellite systems*. Springer International Publishing. Retrieved from https://books.google.fr/books?id=93goDwAAQBAJ

Thorpe, J. (2003). Low-density parity-check (ldpc) codes constructed from protographs. *IPN progress report*, *42*(154), 42–154.

Uchô, A., Healy, C., de Lamare, R., & Souza, R. (2011). Design of ldpc codes based on progressive edge growth techniques for block fading channels. *IEEE Communications Letters*, *15*(11), 1221–1223. https://10.1109/LCOMM.2011.092911.111520

Viterbi, A. (1967). Error bounds for convolutional codes and an asymptotically optimum decoding algorithm. *Information Theory, IEEE Transactions on*, *13*, 260–269. https://10.1109/TIT.1967.1054010

How to cite this article: Ortega L., Poulliat C., GNSS Channel Coding Structures for Fast Acquisition Signals in Harsh Environment Conditions. *Navigation*.